




# Plant Biosynthesis of Zinc Oxide Nanoparticles Using *Punica granatum* L. Extract and its Inhibitory Effect on *Streptococcus mutans*

Sulaiman M. Hasan<sup>1\*</sup> , Luay H. Jalil<sup>2</sup> , Riyam H. Shukur<sup>3</sup> 

1. Department of Basic Science, College of Dentistry, Mustansiriyah University, Baghdad, Iraq
2. College of Dentistry, Al-Farahidi University, Baghdad, Iraq
3. College Engineering, Al-Nahrain University, Baghdad, Iraq

## ABSTRACT

**Background and Aim:** A useful tactic to change membrane permeability, cytoplasmic leakage, and eventual cell death in bacteria is the neutralization of their cell surface potential by nanoscale materials. In this study, pomegranate peel extract was used in an attempt to create biogenic zinc nanoparticles. It is less expensive and uses less hazardous substances than chemical and physical approaches, and is a straightforward substitute for these approaches. Zinc oxide nanoparticles (ZnO NPs) have extensive biological applications. This study was aimed to produce ZnO NPs via a green chemistry approach and analyze their antibacterial capacity.

**Materials and Methods:** ZnO NPs were synthesized by mixing equal volumes of zinc acetate (0.1 M) and pomegranate peel extract. The resulting mixture was heated to 100°C for 180 min and the color change was observed. After several washings of the resulting mixture, ZnO NPs were obtained. The biosynthesized ZnO NPs were characterized using UV-visible spectra, FT-IR spectroscopy, and X-ray diffraction (XRD) spectra. The morphology of ZnO NPs was examined using TEM.

**Results:** The study showed ZnO NPs production in an inexpensive and environmentally friendly way. The ZnO NPs showed optimal antibacterial activity against *Streptococcus mutans*. When the prepared NPs reacted with eugenol, they showed the ability to improve the effectiveness of temporary dental fillings and supplement the oral health outcomes.

**Conclusion:** The ZnO NPs showed favorable antibacterial activity against *S. mutans*. Green synthesis of nanomaterials have emerged as a promising alternative due to their properties against the *S. mutans* responsible for the tooth decay.

**Keywords:** Plant biosynthesis, *Punica granatum* L., *Streptococcus mutans*, Zinc oxide nanoparticles (ZnO NPs)

Received: 2024/03/13;

Accepted: 2024/05/20;

Published Online: 2024/05/25;

## Corresponding Information:

Sulaiman M. Hasan, Department of Basic Science, College of Dentistry, Mustansiriyah University, Baghdad, Iraq Email: [sulaiman.m.hasan@uomustansiriyah.edu.iq](mailto:sulaiman.m.hasan@uomustansiriyah.edu.iq)



Copyright © 2024, This is an original open-access article distributed under the terms of the Creative Commons Attribution-noncommercial 4.0 International License which permits copy and redistribution of the material just in noncommercial usage with proper citation.



Use a device to scan and read the article online

Hasan S M, Jalil L H, Shukur R H. Plant Biosynthesis of Zinc Oxide Nanoparticles Using *Punica granatum* L. Extract and its Inhibitory Effect on *Streptococcus mutans*. Iran J Med Microbiol. 2024;18(2):123-31.

**Download citation:** [BibTeX](#) | [RIS](#) | [EndNote](#) | [Medlars](#) | [ProCite](#) | [Reference Manager](#) | [RefWorks](#)

**Send citation to:**  [Mendeley](#)  [Zotero](#)  [RefWorks](#)

## 1. Introduction

Antibiotic resistance is a challenge we are facing with bacterial pathogens that cause high morbidity and mortality rates. Antibiotic resistant Gram-positive and Gram-negative bacteria have multidrug resistance patterns that make them even resistant to common antibiotics. Due to the lack of efficient prevention measures, the paucity of new antibiotics, and the limited availability of therapies, the situation of today medicine requires the creation of novel treatment alternatives (1). Broad-spectrum antibacterial

properties have been demonstrated by nanoparticles so far.

The most frequently used platform in the modern material science study in the 21<sup>st</sup> century is nanotechnology. The word "nano" stems from a Greek word that means "dwarf." Nanotechnology makes use of formations with dimensions mostly in nanometre scale (1–100 nm). Nanotechnology is becoming a field that is growing quickly because of its applications in science and technology to produce new materials at the nanoscale. One term for nanomaterials in modern

medicine is "wonders." Antibiotics are said to be able to eradicate about six different disease-causing organisms, but nanomaterials are said to be able to eradicate about 650 bacteria (2). Also, antibiotic resistance has increased and there is an unmet need to replace them by more applicable and biocompatible compounds (3).

According to earlier reports, metal nanoparticles (NPs) have been the subject of substantial research due to their unique capabilities, including antibacterial wound healing, optical, electrical, magnetic, and catalytic appliances (4). These features have not been found in bulk phase. The various NPs are employed in many applications; Zinc oxide nanoparticles (ZnO NPs), for example, are widely utilized in sunscreen lotions and cosmetics due to their effective UV-A and UV-B absorption capabilities without dispersing visible light. ZnO NPs have also been applied in agriculture, anticancer treatments, and antibacterial experiments (5). ZnO NPs are being produced at a daily rate, which has led to an increase in unintentional human and animal exposure (6). Environmentally acceptable substitutes for chemical and physical processes in the creation of NPs have been proposed such as microbes, enzymes, plants, and/or plant extracts (7).

Pomegranate peels contain significant amounts of phenolic compounds, such as flavonoids (anthocyanins, catechins, and other complex flavonoids) and hydrolyzable tannins (punicalin, pedunculagin, punicalagin, gallic, and ellagic acid). The peels also have an interior network of membranes that makes up approximately 26–30% of the total weight of the fruit. Pomegranate peel (PoP) and juice contain rich forms of these chemicals, which are responsible for 92% of the fruit antioxidant action (8).

Therefore, there is a need for new green synthesis techniques that are straightforward without the need to a lot of energy or hazardous chemicals. Many studies have been conducted recently to look at the bio-reduction of different metal ions such as Ag, Au, Pd, and Pt into metal NPs. In order to convert metal ions into zero-valence metal NPs, the bio-reduction method takes advantage of the reduction potential of a variety of biochemicals found in natural and renewable materials such as microorganisms and plant extracts. There also have been reports of ZnO green synthesis and their antibacterial capacities (9). Studies have employed zinc nanoparticles against bacteria other than the ones employed in this investigation, such as *S. aureus*, *E. coli*, *K. pneumoniae*, *B. cereus*, *E. faecalis*, *E. faecium*, and *S. pneumonia* (10).

NPs are becoming more and more significant in the scientific research because of their peculiar size and properties. They play a crucial role in many

applications and create tremendous changes in various technological fields (11). Researchers have become increasingly interested in nano-biotechnology in particular. Numerous metal oxide NPs are being developed by nano-biotechnology for use in tissue engineering, pharmaceuticals, medication delivery, cosmetics, and biomedical applications (12, 13). Many researchers are currently striving to create biocompatible medication that is effective in treating both cancer and a variety of infectious disorders (14, 15). Nano-compounds have significant intrinsic characteristics that set them apart from larger particles (16).

Because of their antibacterial properties, NPs are now regarded as nano antibiotics (17). People use NPs in a variety of industrial, health, food, space, chemical, and cosmetics applications, which calls for a green and environmentally friendly approach to their synthesis (18, 19). The aim of this study was to prepare ZnO NPs from pomegranate peels in an inexpensive and environmentally friendly way. The prepared ZnO NPs were tested against *S. mutans*. In their reaction with eugenol, they showed the ability to improve the effectiveness of temporary dental fillings regardless of the tooth condition.

## 2. Materials and Methods

### 2.1. Preparation of plant extract

Pomegranate peels (*Punica granatum* L.) were obtained from a market in Baghdad, washed well, and submerged in water to get rid of the impurities. After that, the veneer was completely air dried to eliminate any remaining moisture. Next, 5 gr of the peels were weighed, chopped, and placed in an oven at 50°C for approximately 1 hr. The dried peels were crushed in a mortar and pestle, and then placed in a beaker by adding 100 ml of deionized water. The resulting mixture was stirred at 60 to 70°C for 1 hr before leaving at room temperature overnight. Whatman No. 1 filter paper was used to filter the extract (Figure 1) (20) and stored at 4°C for further use.

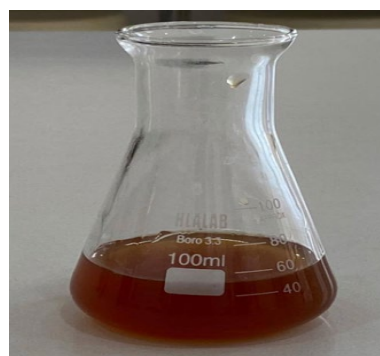
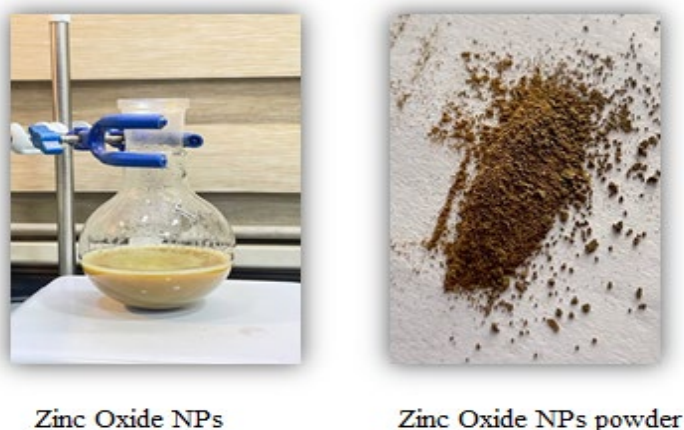


Figure 1. Pomegranate peels extract

## 2.2. Synthesis of ZnO NPs

Zinc acetate solution (100 ml) (0.1 M) was mixed with an equal volume of plant extract solution. The resulting mixture was heated to 80°C for 180 min and the color change was monitored. As seen in [Figure 2](#),

the liquid color changed when the plant excretion came into contact with zinc ions, demonstrating that zinc was absorbed at the nanoscale. As seen in [Figure 2](#), the mixture was heated to 60°C in order to produce the powder form.



**Figure 2.** Synthesis of ZnO NPs

## 2.3. Nanoparticle characterization

The biosynthesized ZnO NPs were described utilizing UV-visible spectra, FT-IR spectroscopy, and X-ray diffraction (XRD) spectra. Also, the morphology of NPs was examined using TEM.

## 2.4. Bacterial media and growth conditions

*Streptococcus mutans* (serotype C) isolated from carious dentine was acquired from Al-farahidi University dental clinics. *S. mutans* was grown for 20 hr at 37°C in an anaerobic environment using brain-heart infusion (BHI) and deMan, Rogosa, and Sharpe (MRS) medium (BD Difco, Franklin Lakes, NJ). Using BHI agar plates supplemented with 1.75 µg/ml polymyxin B, 0.3 U/ml bacitracin, and 0.005% crystal violet, *S. mutans* was selectively isolated.

## 2.5. Method of bacterial growth inhibition

The disk diffusion assay was used to detect the biological activity of the prepared NPs. ZnO NPs were used at 100 µg/L concentration (the highest concentration of the prepared nanocomposite) loaded onto Whatman paper at 37°C and incubated for 24 hr. The resulting diameter of bacterial inhibition was then recorded.

## 2.6. Application of ZnO NPs to dental in vitro

The green synthesized ZnO NPs was mixed with eugenol instead of chemically prepared zinc oxide as a temporary dental filling in the same proportions used in usual methods. Then, the tooth (regardless of tooth condition) was treated in the laboratory in the same way as used to treat tooth decay inside the patient's mouth, as shown in [Figure 3](#).



**Figure 3.** Applications of ZnO NPs to dental in vitro

### 3. Results

#### 3.1 Characterizations of ZnO NPs

##### 3.1.1. UV-visible spectrum

ZnO NPs optical absorption characteristics were examined using UV-vis spectroscopy. Employing a

Shimadzu UV 3600 UV-vis-NIR spectrometer (Kyoto, Japan: Shimadzu Corporation), the sample UV-vis absorption spectra was captured in the 200–1100 nm wavelength range. The production of ZnO NPs was suggested by the peak at 369.12 nm ([Figure 4](#)).

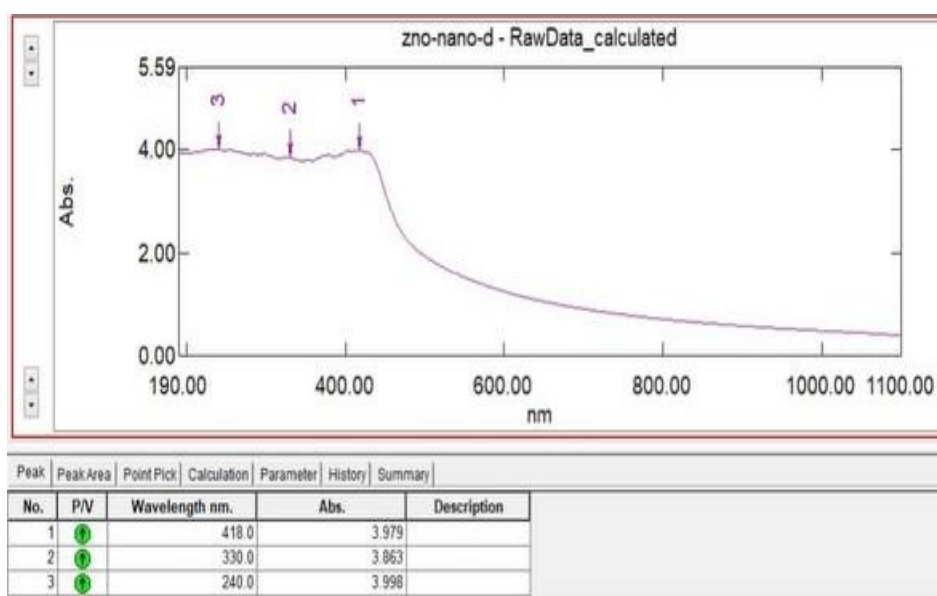


**Figure 4.** UV-visible spectrum of ZnO NPs

##### 3.1.2. FT-IR spectrum

The FT-IR spectrum of powdered ZnO NPs was obtained in the range of 400–4000 cm<sup>-1</sup>. The FT-IR of ZnO NPs was shown in [Figure 5](#).

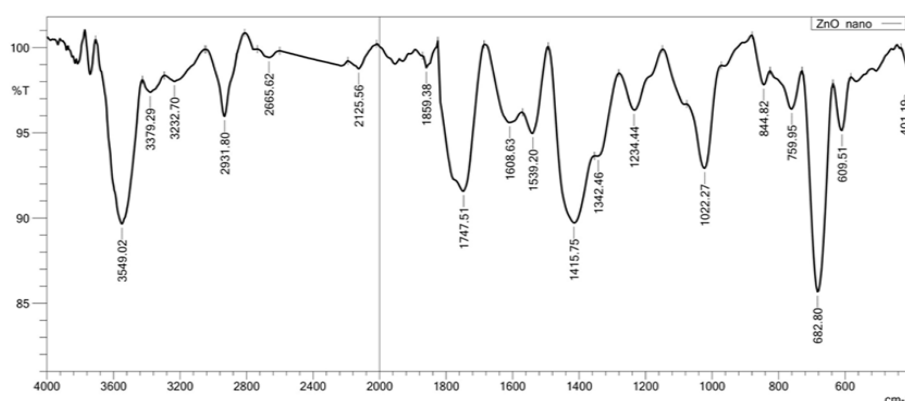


**Figure 5.** FT-IR spectrum

##### 3.1.3 X-ray diffraction analysis

The XRD pattern for the ZnO NPs generated from plant extract was shown in [Figure 6](#). Through XRD examination, the ZnO NPs thickness, phase identity, and crystalline nature were evaluated. The planes (111), (200), and (220) and the peaks at 3 angles

(43.8°, 50.9°, and 74.4°) are all caused by zinc. The XRD analysis confirmed production of ZnO NPs. At angles of 18.3, 24.4, 33.6, 35.2, and 42.7, monoclinic crystallite formation is shown by the XRD analysis by the planes (020), (021), (002), (042), and (131), as shown in [Table 1](#).

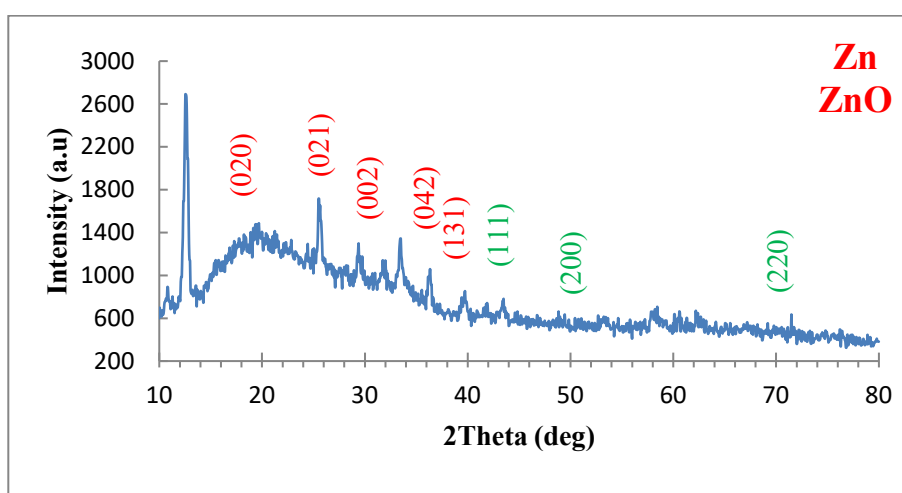


**Figure 6.** XRD spectrum of ZnO NPs

**Table 1.** X-ray diffraction results of ZnO NPs

Sample	2 $\theta$ (Deg.)	hkl	FWHM (Deg.)	$K\lambda$	$\theta = rad$	Cos $\theta$	C.S	Avg.
Zn	43.84	(111)	0.5900	0.1380	0.017	0.928140	14.53623	11.011263
	50.94	(200)	1.1801	0.1380	0.017	0.903390	7.467250	
	74.44	(220)	0.9055	0.1386	0.0174	0.797510	11.03025	
ZnO	18.3	(020)	1.1808	0.1386	0.0174	0.987350	6.832274	19.47941
	24.4	(021)	1.1808	0.1386	0.0174	0.977550	6.900766	
	33.6	(002)	0.1968	0.1386	0.0174	0.957570	42.2684	
	35.2	(042)	0.3444	0.1386	0.0174	0.953470	24.25728	
	42.7	(131)	0.5904	0.1386	0.0174	0.931780	14.47941	

### 3.1.4 Transmission electron microscopy (TEM) evaluation

As shown in [Figure 7](#), transmission electron microscopy (TEM) was used to examine the shape, size, and morphology of the ZnO NPs.

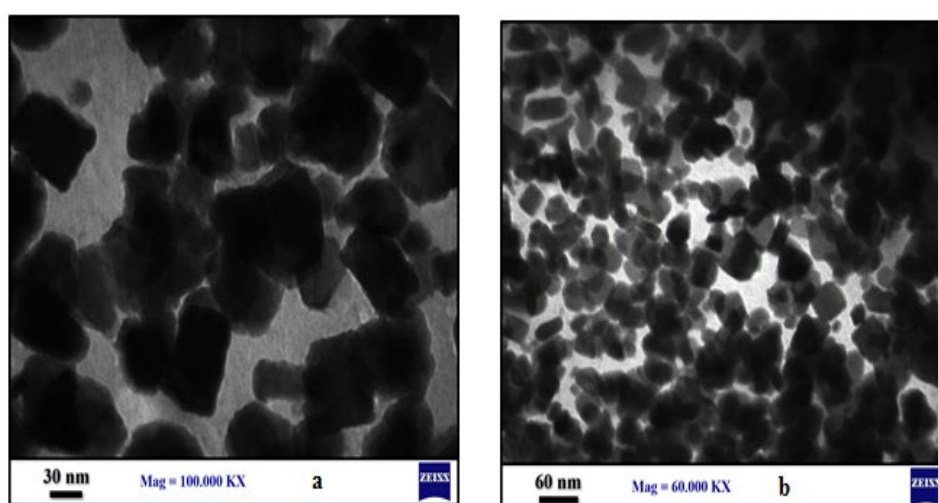


**Figure 7.** TEM images of ZnO NPs (a) 30 nm, (b) 60 nm.



[Figure 7](#) (both a and b) shows TEM images taken at various magnifications (100-200 nm), which showed the appearance of crystalline morphologies with overall average diameters of 30 nm and 60 nm for ZnO NPs.

### 3.1.5 Antimicrobial assay

Disk diffusion assay was performed for the evaluation of antimicrobial activity of ZnO NPs against Gram-positive *S. mutans*. The bacteria were affected by ZnO tiny particles at an intensity of 100% and the percentage of inhibition for *S. mutans* was 29 mm ([Figure 8](#)).

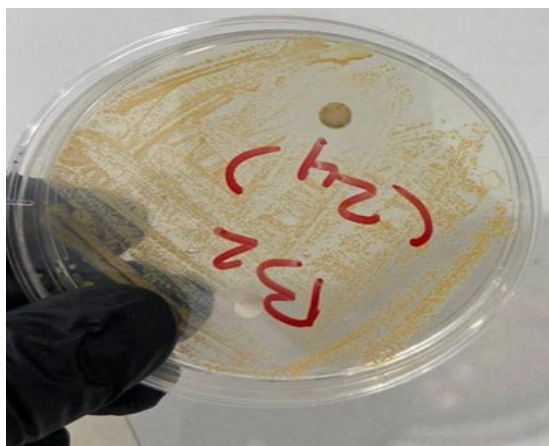


**Figure 8.** Inhibitory effect of ZnO NPs in 100% concentration for *S. mutans*.

## 4. Discussion

In this study, zinc oxide nanoparticles were produced using *Punica granatum* L. extract and its antibacterial effect was assessed against *S. mutans*.

The first indication of plant-based biogenic synthesis of ZnO NPs using *P. granatum* peel aqueous extract is the color shift from dark red to yellowish white. Following a whole day, the highest color change was achieved. It was caused by the activation of plasmon vibrations on the metal and metal oxide-NP surfaces.

UV-Vis spectroscopy was used to identify the maximum absorbance, which is a measure of the maximum SPR unique to ZnO NPs. The collective oscillation of resonant electrons in the conduction band along the electromagnetic field gave rise to SPR peaks in the UV ([21](#)). Here, it was discovered that the phyto-fabricated ZnO NP maximum SPR was 330 nm ([Figure 4](#)). The range of light absorption of ZnO NPs at a wavelength of 350–380 nm is associated with the found absorption peak. The strongest SPR band of ZnO NPs produced by *P. granatum* floral extract was recorded at 345 nm in a recent study ([22](#)). The ZnO NPs made from the aqueous extract of *P. granatum* leaves, on the other hand, showed two peaks at 284 and 357 nm ([23](#)).

[Figure 5](#) illustrates how the final material, ZnO NP, was created using peel aqueous extract and examined using FTIR. The O-H vibration peaks overlapped with the NH vibrations, appearing as a broad band at 3549.02  $\text{cm}^{-1}$  ([24](#)). Zn was produced with various internal small bands at 3379.29 and 3232.70  $\text{cm}^{-1}$ . This attests to the synthesis of primary and secondary amines in addition to OH groups ([25](#)). The Zn control material showed the C-H aliphatic at 2931.80. For ZnO material, thiol stretching bands, which were absent from the control sample, are associated with a peak at 2665.62  $\text{cm}^{-1}$  ([26](#)). The ZnO NPs have a peak at 2125.56  $\text{cm}^{-1}$ , which is associated with the medium sulfonic group stretching bands. The ester group is connected to the ZnO NPs peaks at 1747.51  $\text{cm}^{-1}$ . Additional notable peaks for the ZnO NPs sample were observed at 1437  $\text{cm}^{-1}$  for the organic sulfate groups and carboxylate ions, while the peak at 1539.20  $\text{cm}^{-1}$  is associated with the stretching C-C and the low-intensity NH band of primary amines, indicating that binding with ZnO ions occurred ([27](#)).

The plant aqueous extract has peaks at 1022.27  $\text{cm}^{-1}$ , which are associated with asymmetric C-O-C and C-N stretching. The formation of peaks in the 450–700  $\text{cm}^{-1}$  range, which are absent in the plant aqueous extract, confirms the stretching band of zinc and oxygen and shows that ZnO was successfully formed ([28](#)). The function of different functional groups associated with distinct metabolites in ZnO NPs reduction, capping, and stability was demonstrated by their presence in plant aqueous extract.

The findings of X-ray diffraction on the powder form of phyto-synthesised ZnO NPs in the two theta value ranges of 10–80° are shown in [Figure 6](#). XRD can show the crystalline structure of produced NPs, in accordance with the Joint Committee on Powder Diffraction standard (JCPDS). ZnO NPs were found to exhibit prominent diffraction peaks at two theta values of 18.3°, 24.4°, 33.6°, 35.2°, and 42.7°. These values were correlated with crystal planes of (020), (021), (002), (042), and (131), in that order. XRD chart showed crystalline phyto-synthesized ZnO NPs, as opposed to JCPDS card number 36–1451 ([29](#)). The acquired observations were compatible with previous studies that show the crystalline character of ZnO NPs generated by plant extract, based on XRD diffraction peaks at the same two theta values ([30](#)). The absence of extra peaks on the XRD chart confirmed the high purity of the plant-based ZnO NPs. As previously reported ([22](#)), the broad bases of Bragg XRD peaks show that the sizes of synthesized NPs are small. Using the Debye-Scherrer equation, the crystallite size of ZnO NPs was determined in the current study. Utilizing the maximum diffraction peak of (131), which began

at a  $2^\circ$  value of  $42.7^\circ$ , the measurement was accomplished.

Researchers frequently utilize the TEM to look at the morphology, size, shape, and agglomeration of the NPs. In the current investigation, zinc acetate was efficiently reduced utilizing the peel aqueous extract of *P. granatum* to generate spherical ZnO NPs with minimum aggregation (Figure 7). Furthermore, the average particle size of the ZnO NPs were obtained 30.0 nm by TEM images. The particle size from TEM examination and the crystallite size calculated by XRD using the Debye-Scherrer equation were consistent. The findings supported a previous study result that found ZnO NPs made from *P. granatum* leaf aqueous extract obtained by TEM to be similar in size to those obtained by XRD analysis (31). On the other hand, the TEM analysis revealed the particle size of spherical ZnO NPs, made from an aqueous extract of *Citrus reticulata* peel, ranged from 23 to 90 nm, while the XRD revealed the crystallite size at 8.9 nm (32).

The antibacterial efficacy of ZnO NPs against the studied bacteria was assessed using a disk diffusion assay at 100% concentration; the percentage of inhibition for Gram-positive bacteria *S. mutans* was 29 mm.

## 5. Conclusion

This study confirmed zinc nanoparticles production from pomegranate peels in an inexpensive and environmentally friendly way. ZnO NPs showed optimal and favorable antibacterial activity against *S. mutans*.

## References

1. Larsson DG, Flach CF. Antibiotic resistance in the environment. *Nat Rev Microbiol.* 2022;20(5): 257-69. [DOI:10.1038/s41579-021-00649-x] [PMID] [PMCID]
2. Gunalan S, Sivaraj R, Rajendran V. Green synthesized ZnO nanoparticles against bacterial and fungal pathogens. *Prog Nat Sci Mater Int.* 2012;22(6):693-700. [DOI:10.1016/j.pnsc.2012.11.015]
3. Ramesh M, Anbuvaran M, Viruthagiri GJ. Green synthesis of ZnO nanoparticles using Solanum nigrum leaf extract and their antibacterial activity. *Spectrochim Acta-A: Mol Biomol Spectrosc.* 2015;136:864-70. [DOI:10.1016/j.saa.2014.09.105] [PMID]
4. Abdelbaky AS, Abd El-Mageed TA, Babalghith AO, Selim S, Mohamed AM. Green synthesis and characterization of ZnO nanoparticles using Pelargonium odoratissimum (L.) aqueous leaf extract and their antioxidant, antibacterial and anti-inflammatory activities. *Antioxidants.* 2022; 11(8):1444. [DOI:10.3390/antiox11081444] [PMID] [PMCID]
5. Daniel MC, Astruc D. Gold nanoparticles: assembly, supramolecular chemistry, quantum-size-related properties, and applications toward biology, catalysis, and nanotechnology. *Chem Rev.* 2004;104(1):293-346. [DOI:10.1021/cr030698+] [PMID]
6. Cuenya BR. Synthesis and catalytic properties of metal nanoparticles: Size, shape, support, composition, and oxidation state effects. *Thin Solid Films.* 2010;518(12):3127-50. [DOI:10.1016/j.tsf.2010.01.018]
7. Bhardwaj A, Sharma G, Gupta S. Nanotechnology applications and synthesis of graphene as nanomaterial for nanoelectronics. *Nanomater Environ Biotechnol.* 2020;2020:251-69. [DOI:10.1007/978-3-030-34544-0\_14]

Also, when the ZnO NPs reacted with eugenol, they were shown to have the ability to improve the effectiveness of temporary dental fillings. Green ZnO NPs have emerged as a promising alternative due to their properties against the *S. mutans* commonly responsible for the tooth decay.

## Acknowledgment

We would like to thank our colleagues who contributed to completing this research.

## Ethical Considerations

This study was approved by the Ethics Committee of the College of Dentistry, University of Mustansiriyah (Ethical code. 23, 03.06.2023).

## Authors' Contributions

S.M.H. prepared the plant extract. R.H.S. prepared the nano composite. L.H.J. used the nanocomposite in medical applications.

## Funding

This study was not supported financially by any organization.

## Conflict of Interest

The authors declare no conflicts of interest.

8. Ismail T, Sestili P, Akhtar S. Pomegranate peel and fruit extracts: a review of potential anti-inflammatory and anti-infective effects. *J Ethnopharmacol*. 2012;143(2):397-405. [DOI:10.1016/j.jep.2012.07.004] [PMID]
9. Ifeanyichukwu UL, Fayemi OE, Ateba CN. Green synthesis of zinc oxide nanoparticles from pomegranate (*Punica granatum*) extracts and characterization of their antibacterial activity. *Molecules*. 2020;25(19):4521. [PMID] [PMCID] [DOI:10.3390/molecules25194521]
10. Shivaramakrishnan B, Gurumurthy B, Balasubramanian A. Potential biomedical applications of metallic nanobiomaterials: a review. *Int J Pharm Sci Res*. 2017;8(3):985.
11. Luyts K, Napierska D, Nemery B, Hoet PH. How physico-chemical characteristics of nanoparticles cause their toxicity: complex and unresolved interrelations. *Environ Sci Process Impacts*. 2013;15(1):23-38. [DOI:10.1039/C2EM30237C] [PMID]
12. Rauta PR, Mohanta YK, Nayak D, editors. *Nanotechnology in biology and medicine: research advancements & future perspectives*. CRC Press: Florida, U.S. 2019. [DOI:10.1201/9780429259333] [PMCID]
13. Alamdari S, Mirzaee O, Jahroodi FN, Tafreshi MJ, Ghamsari MS, Shik SS, et al. Green synthesis of multifunctional ZnO/chitosan nanocomposite film using wild *Mentha pulegium* extract for packaging applications. *Surf Interface*. 2022;34:102349. [DOI:10.1016/j.surf.2022.102349] [PMID] [PMCID]
14. Ni B, Shi Y, Wang X. The sub-nanometer scale as a new focus in nanoscience. *Adv Mater*. 2018;30(43):1802031. [DOI:10.1002/adma.201802031] [PMID]
15. Asha AB, Narain R. *Nanomaterials properties*. In *Polymer science and nanotechnology*. Elsevier: Edmonton, Canada. 2020. pp. 349-59. [DOI:10.1016/B978-0-12-816806-6.00015-7]
16. Dolai J, Mandal K, Jana NR. Nanoparticle size effects in biomedical applications. *ACS Appl. Nano Mater*. 2021;4(7):6471-96. [DOI:10.1021/acsanm.1c00987]
17. Fernandez-Garcia M, Martinez-Arias A, Hanson JC, Rodriguez JA. Nanostructured oxides in chemistry: characterization and properties. *Chem Rev*. 2004;104(9):4063-104. [DOI:10.1021/cr030032f] [PMID]
18. Patil MP, Kim GD. Eco-friendly approach for nanoparticles synthesis and mechanism behind antibacterial activity of silver and anticancer activity of gold nanoparticles. *Appl Microbiol Biotechnol*. 2017;101:79-92. [DOI:10.1007/s00253-016-8012-8] [PMID]
19. Omran BA. *Nanobiotechnology: a multidisciplinary field of science*. Springer Nature: Berlin, Germany. 2020. pp. 145-84. [DOI:10.1007/978-3-030-46071-6]
20. Madkour LH. *Nanoelectronic Materials: Fundamentals and Applications*. Springer Nature: Cham, Switzerland; 2019. [DOI:10.1007/978-3-030-21621-4]
21. Salem SS, El-Belely EF, Niedbała G, Alnoman MM, Hassan SE, Eid AM, et al. Bactericidal and in-vitro cytotoxic efficacy of silver nanoparticles (Ag-NPs) fabricated by endophytic actinomycetes and their use as coating for the textile fabrics. *Nanomaterials*. 2020;10(10):2082. [DOI:10.3390/nano10102082] [PMID] [PMCID]
22. Templeton AC, Pietron JJ, Murray RW, Mulvaney P. Solvent refractive index and core charge influences on the surface plasmon absorbance of alkanethiolate monolayer-protected gold clusters. *J Phys Chem B*. 2000;104(3):564-70. [DOI:10.1021/jp991889c]
23. Fouda A, Saied E, Eid AM, Kouadri F, Alemam AM, Hamza MF, et al. Green synthesis of zinc oxide nanoparticles using an aqueous extract of punica granatum for antimicrobial and catalytic activity. *J Funct Biomater*. 2023;14(4):205. [DOI:10.3390/jfb14040205] [PMID] [PMCID]
24. Hamza MF, Wei Y, Althumayri K, Fouda A, Hamad NA. Synthesis and characterization of functionalized chitosan nanoparticles with pyrimidine derivative for enhancing ion sorption and application for removal of contaminants. *Materials*. 2022;15(13):4676. [DOI:10.3390/ma15134676] [PMID] [PMCID]
25. Zahra MH, Hamza MF, El-Habibi G, Abdel-Rahman AA, Mira HI, Wei Y, Alotaibi SH, Amer HH, Goda AE, Hamad NA. Synthesis of a novel adsorbent based on chitosan magnetite nanoparticles for the high sorption of Cr (VI) ions: A study of photocatalysis and recovery on tannery effluents. *Catalysts*. 2022;12(7):678. [DOI:10.3390/catal12070678]
26. Hamza MF, Wei Y, Khalafalla MS, Abed NS, Fouda A, Elwakeel KZ, et al. U (VI) and Th (IV) recovery using silica beads functionalized with urea-or thiourea-based polymers-Application to ore leachate. *Sci Total Environ*. 2022;821:153184. [DOI:10.1016/j.scitotenv.2022.153184] [PMID]



27. Hamza MF, Lu S, Salih KA, Mira H, Dhmees AS, Fujita T, et al. As (V) sorption from aqueous solutions using quaternized algal/polyethyleneimine composite beads. *Sci Total Environ.* 2020;719:137396. [DOI:10.1016/j.scitotenv.2020.137396] [PMID]
28. Mohamed AA, Fouda A, Abdel-Rahman MA, Hassan SE, El-Gamal MS, Salem SS, et al. Fungal strain impacts the shape, bioactivity and multifunctional properties of green synthesized zinc oxide nanoparticles. *Biocatal Agric Biotechnol.* 2019;19:101103. [DOI:10.1016/j.bcab.2019.101103]
29. Singh K, Singh J, Rawat M. Green synthesis of zinc oxide nanoparticles using Punica Granatum leaf extract and its application towards photocatalytic degradation of Coomassie brilliant blue R-250 dye. *SN Appl Sci.* 2019;1:1-8. [DOI:10.1007/s42452-019-0610-5]
30. Vijayaraghavan K, Ashokkumar T. Plant-mediated biosynthesis of metallic nanoparticles: A review of literature, factors affecting synthesis, characterization techniques and applications. *J Environ Chem Eng.* 2017;5(5):4866-83. [DOI:10.1016/j.jece.2017.09.026]
31. Gur T, Meydan I, Seckin H, Bekmezci M, Sen F. Green synthesis, characterization and bioactivity of biogenic zinc oxide nanoparticles. *Environ Res.* 2022;204:111897. [DOI:10.1016/j.envres.2021.111897] [PMID]
32. Rafique M, Sohaib M, Tahir R, Bilal Tahir M, Rizwan M. Plant-mediated green synthesis of zinc oxide nanoparticles using peel extract of citrus reticulata for boosting seed germination of brassica nigra seeds. *J Nanosci Nanotechnol.* 2021;21(6):3573-9. [DOI:10.1166/jnn.2021.19015] [PMID]